PCCP

PAPER

Cite this: *Phys. Chem. Chem. Phys.*, 2019, **21**, 22947

The effect of ionic strength and phosphate ions on the construction of redox polyelectrolyte–enzyme self-assemblies

Daniele Zappi,[ab] Lucy L. Coria-Oriundo,[ac] Esteban Piccinini,[d] Marcos Gramajo,[a] Catalina von Bilderling,[de] Lía I. Pietrasanta,[ef] Omar Azzaroni *[d] and Fernando Battaglini *[a]

Received 18th July 2019,
Accepted 29th September 2019

DOI: 10.1039/c9cp04037d

rsc.li/pccp

Layer by layer assembly of polyelectrolytes with proteins is a convenient tool for the development of functional biomaterials. Most of the studies presented in the literature are based on the electrostatic interaction between components of opposite charges, limiting the assembly possibilities. However, this process can be tuned by modifying the environment where the main constituents are dissolved. In this work, the electron transfer behavior between an electroactive polyelectrolyte (polyallylamine derivatized with an osmium complex) and a redox enzyme (glucose oxidase) is studied by assembling them in the presence of phosphate ions at different ionic strengths. Our results show that the environment from which the assembly is constructed has a significant effect on the electrochemical response. Notably, the polyelectrolyte dissolved in the presence of phosphate at high ionic strength presents a globular structure which is preserved after adsorption with substantial effects on the buildup of the multilayer system, improving the electron transfer process through the film.

Introduction

Supramolecular assembly generated by layer-by-layer (LbL) deposition is a powerful method for the construction of multicomponent architectures at a nanometric level in diverse fields such as hydrophobic interfaces,[1] self-healing textiles,[2] membranes with selective permeation rates,[3] or electron transfer processes.[4–8] The main idea behind the LbL technique is the alternative deposition of two species with opposite charge; however, the environment from which the assembly is grown plays a crucial role in the structure and properties of the film since other types of interactions participate, such as hydrogen-bonding, hydrophobic interactions, and specific interactions (*e.g.*, avidin–biotin, lectin–carbohydrate).[9] For example, the self-assembly of a positively charged weak polyelectrolyte such as polyallylamine (PA) with surfactants such as dodecylsulfate, octodecylsulfate, and dodecylphosphate produces different ordered structures,[4,6,10] while polyelectrolyte solutions in the presence of small ions of different charges and at different ionic strength produce a great diversity of assemblies. The observed structures are in part due to the fact that the chain conformation of polyelectrolytes is strongly influenced by their environment. For example, Lösche *et al.* observed in the construction of polyallylamine/polystyrenesulfonate (PA/PSS) films from solutions with different NaCl concentrations a direct relationship between the NaCl concentration and the multilayer structure; as the ionic strength grows, a linear increase of the film thickness is observed.[11] On the other hand, Dressick *et al.* studied the effect of the ion type, especially divalent anions (*e.g.* SO_4^{2-}, HPO_4^{2-}), on the assembly of polyelectrolyte multilayers by building PA/PSS multilayer films from aqueous solutions containing these anions at concentrations below 50 mM and in the presence of a high concentration of sodium chloride (1 M) to enhance the effect of the anion type by the electrostatic effect,[12] while polyelectrolytes and surfactants of the same charge can be assembled in the presence of an excess of ions.[13] More recently, lysozyme was integrated into an LbL assembly by surrounding it with polystyrenesulfonate at different conditions of pH and ionic strength to tune the amount of protein deposited and the hydration level.[14]

[a] *INQUIMAE (CONICET), Departamento de Química Inorgánica, Analítica y Química Física, Facultad de Ciencias Exactas y Naturales, Universidad de Buenos Aires, Ciudad Universitaria, Pabellón 2, C1428EHA Buenos Aires, Argentina. E-mail: battagli@qi.fcen.uba.ar*
[b] *Department of Chemistry, University of Rome "La Sapienza", p.le A. Moro, 5, 00185 Rome, Italy*
[c] *Facultad de Ciencias, Universidad Nacional de Ingeniería, Av. Túpac Amaru 210, Lima 25, Peru*
[d] *Instituto de Investigaciones Fisicoquímicas Teóricas y Aplicadas (INIFTA), (UNLP, CONICET), Sucursal 4, Casilla de Correo 16, 1900 La Plata, Argentina. E-mail: azzaroni@inifta.unlp.edu.ar*
[e] *Departamento de Física, Facultad de Ciencias Exactas y Naturales, Universidad de Buenos Aires, C1428EHA Buenos Aires, Argentina*
[f] *Instituto de Física de Buenos Aires (IFIBA), (UBA, CONICET), C1428EHA Buenos Aires, Argentina*

It is evident that in all these examples, the type of ions and the ionic strength produce striking changes in the obtained film. In this context, one of the most studied polyelectrolytes, as it can be observed from the previous examples, is polyallylamine, since it presents a flexible and lineal backbone, it can change its charge as function of pH, and the presence of the amino groups allows interaction with other species through hydrogen bonds, and they can be chemically modified. All these features make polyallylamine a suitable candidate for different applications: drug release,[15–17] sensor construction,[18,19] fuel cells,[20,21] and selective filtration,[22,23] among others.

The LbL methodology has been used to build systems which resemble biological structures in which the interaction between amines and phosphate anions plays a crucial role in the assembly.[24–27] Inspired by these studies and by our previous experience in the study of the electron transfer process between PA derivatized with polypyridyl osmium complexes (OsPA) and redox enzymes,[28–30] we decided to study the effect of phosphate ions in the assembly of OsPA with glucose oxidase (GOx) as model system to establish the effect of this ion on the film structure and its consequences for the electron transfer process, since the combination of this electroactive polyelectrolyte with enzymes makes this system an excellent option for the construction of sensors and biofuel cells. In this work, we present the buildup of OsPA and GOx multilayer systems in the presence of phosphate ions at low (0.1 M) and high (1 M) ionic strength given by NaCl. The presence of phosphate ions at high ionic strength produces a globular structure on the polyelectrolyte, which is preserved after adsorption, changing the ratio in which OsPA and GOx build up the multilayer system and therefore the electron transfer process.

Experimental section

Reagent and materials

$OsCl_6(NH_4)_2$, pyridine aldehyde 97% and polyallylamine were purchased from Aldrich; 2,2′-bipyridine was purchased from Fluka, and glucose oxidase was from Roche. All other reagents were of analytical grade. The complex $[Os(bpy)_2Cl(PyCOH)]Cl$ (PyCOH = pyridine-4-aldehyde) and osmium-modified polyallylamine (OsPA) were prepared as previously reported.[31] The stoichiometry ratio between the osmium complex and allylamine monomer was 1 : 60. All solutions used in this work have been prepared using MilliQ water.

OsPA or GOx was dissolved at a final concentration of 2 mg mL^{-1} in the solutions listed in Table 1.

Table 1 Nomenclature used in this work

Solution name	Solution composition
HIS	1.00 M NaCl
Pi,HIS	11 mM K_2HPO_4 + 10 mM KH_2PO_4 + 1.00 M NaCl
LIS	0.10 M NaCl
Pi, LIS	11 mM K_2HPO_4 + 10 mM KH_2PO_4 + 0.10 M NaCl

All solutions were adjusted to pH = 6.1.

Graphite electrode modification

An in-house constructed screen printed 3-electrode system was used.[32] Before the multilayer assembly, the working electrodes were activated by applying 1 V *vs.* Ag/AgCl for 60 seconds in the presence of 0.1 M NaCl and rinsed with milliQ water. The working electrodes were sequentially exposed to 15 μL of the OsPA and GOx solutions left for 20 minutes in a closed container with controlled humidity (92% RH, controlled with a potassium nitrate saturated solution). Then, the electrodes were rinsed, first with a solution having the same salt composition as the deposition solution and afterward with milliQ water; finally, they were dried with a flow of nitrogen and used for the electrochemical experiments.

Quartz balance measurements (QCM-D)

The QCM-D experiments were performed using a Q-Sense instrument (QCM-D, Q-Sense E1, Sweden) equipped with Q-Sense Flow Module (QFM 401). For all measurements, QSX 301 gold sensors were used. Samples were perfused using a peristaltic microflow system (ISMATEC, ISM 596D Glattbrugg, Switzerland). Gold sensors were activated with O_3 and UV for 15 min immediately before use. All experiments were performed in flow mode with a flow rate of 100 μL min^{-1} at 25.0 °C. The gold sensor was modified with 20 mM cystamine for 1 hour. The first layer of OsPA was generated from a solution containing only 5 mM phosphate solution at pH 7, then the rest of the layers were deposited with the previously described OsPA and GOx solutions. In all the cases, they flowed for 4 minutes, then the flow was stopped, and each solution was left in contact with the gold sensor for 20 minutes. After, the solution was removed by flowing a solution with the same ion composition without OsPA or GOx, until signal stabilization was achieved.

Electrochemical experiments

All electrochemical experiments were carried out in a solution containing 50 mM HEPES + 100 mM NaCl buffer solution at pH 7.0 or in 100 mM glucose in 50 mM HEPES + 100 mM NaCl using a Gamry potentiostat (Gamry Interface 1000, Gamry Instruments, USA).

Dynamic light scattering measurements

The hydrodynamic diameter and z-potential of the colloids were determined by Dynamic Light Scattering employing a Zetasizer Nano (ZEN3600, Malvern, UK) configured in the backscattered detection optic arrangement, that is the detector at 7° to the incident light beam, a 633 nm He–Ne laser and a temperature of 25 °C.

For the zeta potential calculations, the Smoluchowski approximation of the Henry equation was employed. Measurements were performed in triplicate using disposable capillary cells (DTS 1061 1070, Malvern) with a cell driving voltage of 30 V.

Atomic force microscopy

AFM images were acquired with a Multimode 8 AFM (Nanoscope V Controller, Bruker, Santa Barbara, CA). Tapping mode imaging was conducted in buffer solution (50 mM HEPES + 100 mM NaCl)

by using V-shaped silicon nitride AFM probes (SNML, 0.07 N m^{-1} spring constant, 2 nm nominal tip radius, Bruker). Each sample was imaged at different locations on the substrate to ensure reproducibility. The AFM images were processed using Nanoscope software (Bruker) to remove the background slope.

Nomenclature

For clarity, we employ the following shorthand to identify the different solutions used in the buildup process: X@Y, where X represents OsPA or GOx and Y represents the medium where they are dissolved (Table 1); for example OsPA@Pi,HIS represents OsPA dissolved in a phosphate solution at high ionic strength (second entry in Table 1).

We use the following convention for multilayers: $(OsPA/GOX)_n$, where n is the number of layer pairs. $(OsPA/GOX)_n$@Y represents a multilayer grown from a Y solution. For example, $(OsPA/GOX)_5$@Pi,HIS represents a system of 5 bilayers constructed from OsPA and GOx solutions containing phosphate at high ionic strength.

Results and discussion

In contrast to previous studies where electroactive polyallylamine–enzyme assembly was carried out on gold, the electrochemical studies presented here were carried out on previously oxidized screen-printed graphite electrodes (SPE). These electrodes were exposed for 20 minutes to an OsPA@Pi,HIS solution. The negatively charged counterpart for the assembly construction was glucose oxidase under the same conditions (GOx@Pi,HIS). The electrochemical response of these modified electrodes was studied by cyclic voltammetry in 50 mM HEPES buffer (pH = 7.0, 0.10 M NaCl) or 0.10 M glucose in the same buffer. The same construction was carried out from solutions without phosphate at the same pH as a control experiment (X@HIS, where X can be OsPA or GOx).

Fig. 1 (top) shows the results obtained for $(OsPA/GOX)_5$@Pi,HIS. The peak current densities can be attributed to the amount of OsPA adsorbed. This result resembles the one obtained by Dressick *et al.*, where divalent ions can form thicker layers on glass and quartz for the PA/PSS system.[12] It can be observed that the $(OsPA/GOX)_n$@HIS system presents an erratic response, while the one containing phosphate ions can steadily grow.

The same electrodes have been tested in the presence of glucose to evaluate the GOx catalytic properties. The obtained results are shown in Fig. 1 (middle). The effect of the anion involved in the assembly is further magnified in the presence of glucose: the catalytic response for $(OsPA/GOX)_5$@Pi,HIS shows minimum hysteresis (Fig. 1, bottom), suggesting an outstanding interaction between the two active redox centers (osmium complex and FAD) and the ability of glucose to freely diffuse through the film. No catalysis is observed for the system without phosphate, showing the difficulty of building up the polyelectrolyte–protein multilayer system at high ionic strength since the salt concentration controls the range and strength of the electrostatic interactions, one of the main driving forces in the assembly process involving proteins.[33] Taking into account that for thin

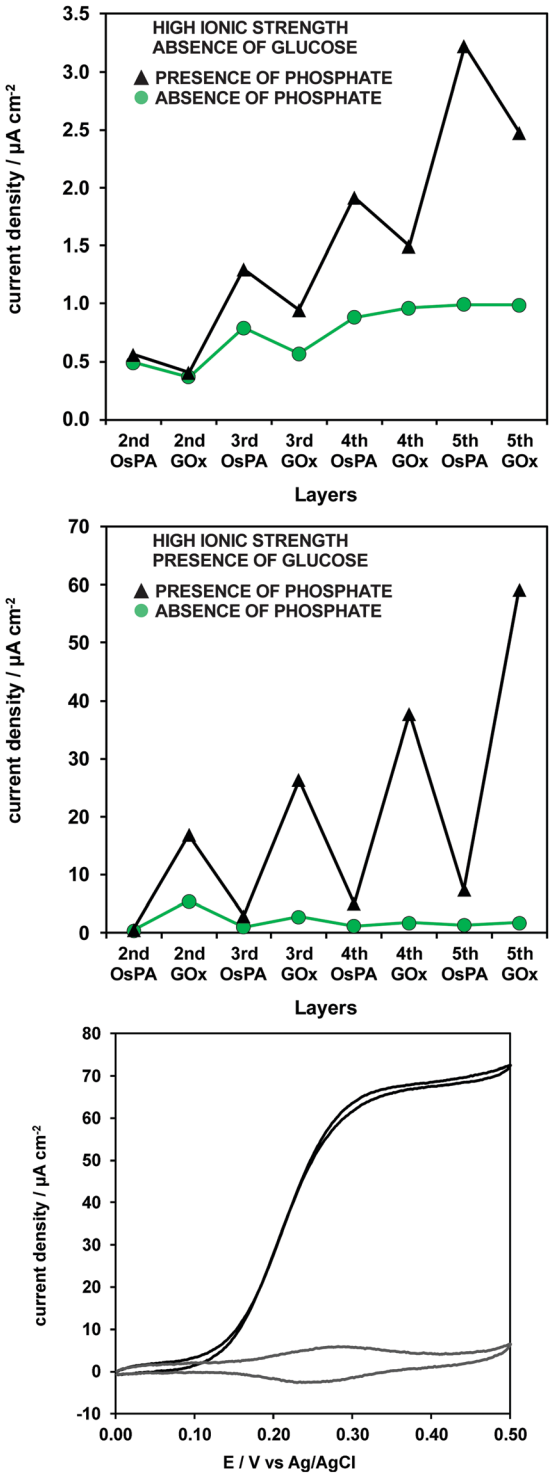

Fig. 1 Current densities for cyclic voltammetry carried out at 10 mV s^{-1} after deposition of each layer on SPE electrodes at high ionic strength (1 M NaCl). Layers constructed in the presence of phosphate (triangles), and in the absence of phosphate (circles). At the top, experiments performed in 50 mM HEPES buffer + 0.1 M NaCl, pH = 7.0. In the middle, experiments performed in 100 mM glucose (50 mM HEPES buffer + 0.1 M NaCl, pH = 7.0). The current densities are the average of three independent electrodes for each case. At the bottom, cyclic voltammetry for $(OsPA/GOX)_5$@Pi,HIS. In gray, in the absence of glucose; in black, in the presence of glucose.

films the electrochemical response for the saturated glucose electrode scales linearly with the redox mediator and the enzyme concentration,[34] higher adsorption of OsPA due to the presence of phosphate allows higher adsorption of the enzyme.

A behavior that deserves attention is the effect of the outmost layer on the electrochemical response, which has been previously observed in polyallylamine modified with osmium[8] or ferrocene[35] redox centers. However, there is no conclusive model to explain this behavior. Several steps are involved in this process: electron transfer at the electrode/film interface, electron hopping between the redox centers in the film, counterion diffusion inside the film and ion exchange at the film/solution interface. Changes in the electron transfer rate in the electrode/polyelectrolyte interface can be ruled out since the peak potential separation is practically the same in all cases; the same can be considered for ion diffusion inside the film. Regarding ion exchange in the film/solution interface, Liu and Anzai[35] have proposed that a positively terminated film facilitated anion transport during the redox process. In coincidence with Calvo *et al.*,[8] we consider that in our case important changes are produced in the segmental movement of the osmium centers after the GOx adsorption, affecting the electron hopping mechanism. GOx fills voids or empty spaces left by the OsPA colloids, which can decrease the flexibility of the system and act as an insulator among redox centers, decreasing the current observed in the absence of glucose. In the presence of glucose, the analysis of the catalytic current behavior becomes more complex, since the glucose oxidation and the enzyme regeneration reactions involve freely diffusing species and extra immobilized redox centers (FAD). However, now GOx becomes a species able to exchange electrons with the osmium redox centers, thus improving the electron transfer process when glucose is present. This result differs from those observed for a similar system built at low ionic strength where the catalytic current decreases when GOx is the last layer. Also, a striking decrease in the catalytic current is observed when the polyelectrolyte is the last layer. A possible explanation for this observation is a change in the pH in the outmost layers of the film, affecting the enzymatic kinetics since the interaction between phosphate and amino groups is able to introduce changes in the proton concentration.[36]

Several examples of (OsPA/GOx) multilayer systems are reported in the literature;[7,8] where OsPA and GOx are dissolved in water and the pH is adjusted by a minimum amount of acid or base. These systems grown at very low ionic strength present an increasing electrochemical response as the number of layer increases. The results obtained here for $(OsPA/GOX)_n$@HIS show that the growth of the system is hindered by the screening effect at high ionic strength, while the introduction of phosphate under the same conditions allows the interaction of OsPA and GOx by a different mechanism.

Since phosphate appears to be the component producing the main changes in the electrochemical response, we proceeded to carry out the same OsPA/GOx LbL construction using the phosphate ion at the same pH and concentration in a solution containing a lower NaCl concentration (0.1 M) (X@Pi,LIS; where X is OsPA or GOx). As can be seen, in Fig. 2 (top), in the absence of

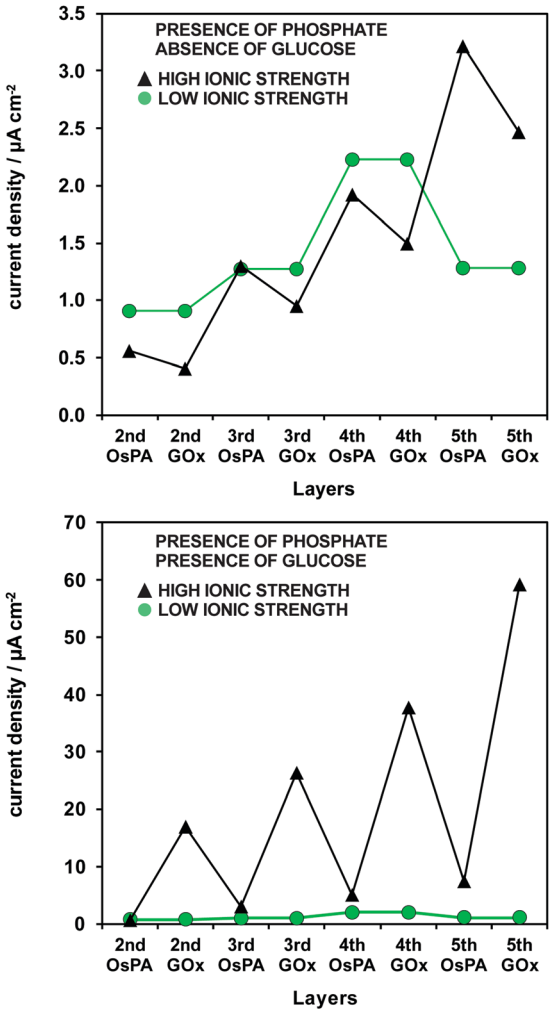

Fig. 2 Current densities for cyclic voltammetry carried out at 10 mV s^{-1} after deposition of each layer on SPE electrodes at low (circles) and high (triangles) ionic strength in the presence of phosphate. Top: Peak current responses in 0.1 M NaCl + 50 mM HEPES buffer, pH = 7.0. Bottom: Catalytic currents observed for 100 mM glucose in 0.1 M NaCl in 50 mM HEPES buffer, pH = 7.0. The voltammetry reported in both graphs was performed at a 10 mV s^{-1} scan rate.

glucose the electrochemical responses of the two electrodes sharply differ: while the electrodes modified at high ionic strength show the behavior discussed before (triangles), the electrodes prepared at lower ionic strength do not show a remarkable variation in the electrochemical response after each OsPA layer (circles). The difference between the electrodes prepared with different ionic strength solutions is even more marked in the presence of glucose (Fig. 2, bottom): electrodes prepared with the lower ionic strength solutions show negligible catalytic activity. In these conditions, the incorporation of GOx seems hindered by the presence of phosphate. Similar behavior was already observed for the formation of polyallylamine/polyacrylate multilayers where the adsorption process in the presence of phosphate is very slow or completely inhibited, depending on its concentration, a fact attributed to the complexation between phosphate and amine groups.[37] In our case, a rinsing effect is observed as the number of

layers increased, yielding a decrease in current. Another example of this behavior is given by the adsorption of GOx onto PA in the presence of phosphate ions at pH 7.4 in 0.1 M KCl, showing that the protein scarcely adsorbs in the presence of phosphate at concentrations higher than 10 mM.[24]

The film growth at high ionic strength can be explained by the change in the polyelectrolyte structure and the interaction with its surroundings. On the one hand, phosphate is able to promote polyelectrolyte intra- and intermolecular bridging, generating stable particles in solution, and on the other hand, chloride ions act as mild chaotropic anions, interacting with the polyelectrolyte and in turn reducing its solvation; therefore, thus improving its adsorption on the surface. This effect becomes more significant at high ionic strength. The chaotropic effect was already studied by Salomäki *et al.*[38] for polyelectrolyte multilayers built in the presence of monovalent anions, showing that their chaotropic character induces deposition and a loopy structure. Also, the growth of polyallylamine and polystyrene sulfonate layers under the same conditions used in this work produces the thickest films in a comprehensive study carried out with different polyvalent anions at high ionic strength.[12]

The catalytic response in the cyclic voltammetry presented in Fig. 1 (bottom) shows two remarkable features: the forward and backward traces are practically the same, and the catalytic current is *ca.* 59 μA cm^{-2}. This represents an optimum relationship between OsPA and GOx since in previous constructions lower density currents were obtained,[7] or mixed kinetics/diffusion control is manifested by the presence of a peak current and hysteresis between the forward and backward traces.[10]

Quartz crystal microbalance with dissipation is a useful technique to characterize self-assembled systems, allowing one to know the amount of material incorporated in each layer and its viscoelastic behavior, so comparisons regarding the composition of the film can be made. Several studies describing the construction of osmium derivatized polyallylamine assemblies under different conditions characterized them using this technique.[8,10,28]

As OsPA does not directly adsorb on the gold surface, we adopted the same strategy as Marmisollé *et al.*[39] where gold was previously modified with cysteamine, and then the exposure to OsPA was carried out in a solution containing only 5 mM phosphate; further depositions were carried out in the presence of phosphate at high ionic strength (@Pi,HIS). The dissipation/frequency shift ratio ($\Delta D/-\Delta F$) increased from 0.1 to 0.47 × 10^{-6} Hz^{-1}, indicating that as the thickness of the film grows, the film loses rigidity; however, the Sauerbrey equation still can be applied with a good approximation.[40] The results can be observed in Fig. 3 (white symbols), where always the amount of deposited OsPA is higher than the GOx, with a ratio OsPA/GOx of around 1.3 for the second and third layers, and 2.3 for the fourth and fifth layers. This result is in contrast to those carried out at very low ionic strength,[7,8] where the OsPA/GOx ratio is smaller than 0.2. Finally, the assembly in the presence of phosphate at low ionic strength (@Pi,LIS) shows an erratic behavior (data not shown) similar to the peak currents observed

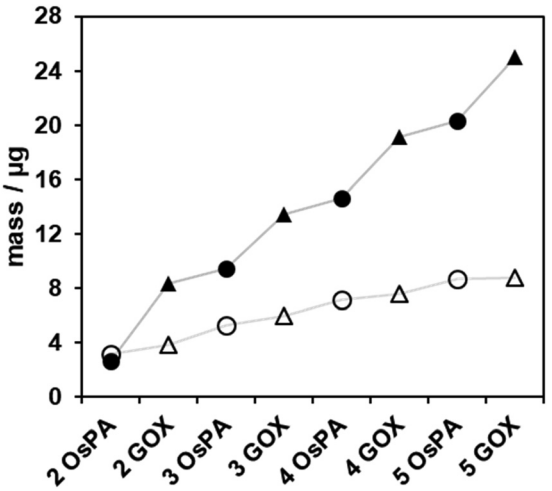

Fig. 3 The adsorbed mass determined by QCM for the assembly of OsPA/GOx under different conditions. $(OsPA/GOX)_n$@Pi,HIS: OsPA layer (white circles); GOx layer (white triangles). $(OsPA@Pi,HIS/GOX@H_2O)_n$: OsPA layer (black circles); GOx layer (black triangles). Grey lines are only for eye guidance. All solutions are at pH 6.1.

in Fig. 2 (top) and in accordance with the phosphate rinsing effect already observed.[24]

Comparing the amount of OsPA and GOx adsorbed in our experiments to those carried out in water, it can be observed that the amount of OsPA adsorbed is similar, while the amount of GOX is eight times higher in their case; however, the catalytic currents are similar for both experiments.

These results drove us to study the effect on the assembly using GOx dissolved in water, adjusting the pH to 6.1 with a minimum amount of HCl (GOx@H_2O), and maintaining the OsPA in phosphate at high ionic strength (OsPA@Pi,HIS). The QCM results show that the amount of OsPA adsorbed is practically the same, while the adsorbed GOx increases from

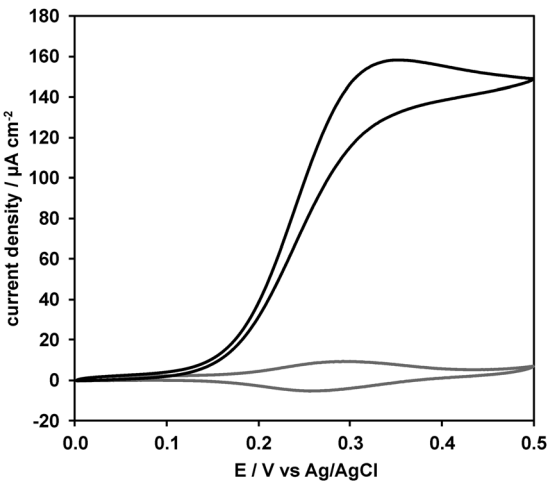

Fig. 4 Cyclic voltammetry for the same system built from OsPA@Pi,HIS and GOx@H_2O (five layers). In gray, in the absence of glucose (0.1 M NaCl + 50 mM HEPES buffer, pH = 7.0); in black, in the presence of glucose (100 mM glucose in 0.1 M NaCl in 50 mM HEPES, pH = 7.0).

an average value of 1 to 4.5 μg cm^{-2} in each step (Fig. 3, black symbols), with an improving effect on the electrochemical response, where a catalytic current of 148 μA cm^{-2} is observed (Fig. 4), meaning an increase of more than two over the system $(OsPA/GOx)_5$@Pi,HIS (Fig. 1, bottom). On the other hand, the voltammogram shows features (peak current, hysteresis) that can be related to some limitations in the diffusion of glucose or the efficiency of the electron hopping process due to the larger amount of enzyme.

For polyelectrolytes, it is known that the deposited layer structure is influenced by the ionic strength of the precursor solution, a behavior already observed for polyallylamine.[11]

Dynamic light scattering (DLS) experiments for OsPA@Pi,HIS and OsPA@HIS solutions show a change in the phase behavior of the polyelectrolyte (Table 2). In the presence of phosphate, the polyelectrolyte produces aggregates with some polydispersity that present two size distributions with diameters of 7 and 16 nm, while in the absence of phosphate no aggregates can be observed. Therefore, we can consider the formation of a globular structure in the presence of phosphate due to the interactions with the primary amino groups in the polyelectrolyte and a random-coil structure in its absence due to the shielding effect of the high ionic strength, affecting the further assembly. On the other hand, a DLS experiment carried out for GOx@Pi,HIS shows a similar hydrodynamic diameter to that in water.[41]

Table 2 Particle diameter and zeta potential obtained by DLS

Sample	Diameter/nm	Zeta potential/mV
OsPA@HIS	3.4 ± 0.9	
OsPA@Pi,HIS[a]	7 ± 1/16 ± 5	8 ± 3
GOx@Pi,HIS	11 ± 2	−2 ± 3

[a] 99% of the particles are within two distributions of particles of different diameter (7 and 16 nm).

As the adsorption process for OsPA@Pi,HIS generates striking changes in the electrochemical response, the structure of the polyelectrolyte, once it is adsorbed, was studied by atomic force microscopy. Fig. 5 shows *in situ* AFM images of the $(OsPA/GOx)_n$@Pi,HIS samples taken at different deposition layers. A nodular structure homogeneously distributed on the surface is observed for different deposition layers either with OsPA or GOx as the outermost layer. The homogeneous structure observed here contrasts with those previously observed for polyallyamine assembled with proteins. For example, Flexer *et al.*[7] observed more irregular films for polyallylamine–GOx self-assembled films constructed from solutions at different pH at low ionic strength. A similar result was found by Caruso *et al.*[42] for the adsorption of anti-IgG when the interlayer between anti-IgG layers is poly(4-styrenesulfonate), which the authors attribute to the aggregation of the protein. Here the globular structure proposed from DLS results seems to assemble in a homogenous architecture with voids through which species could diffuse, which are evident in high resolution topography images of the samples from the first layers (see the arrows in the zoomed image in Fig. 5).

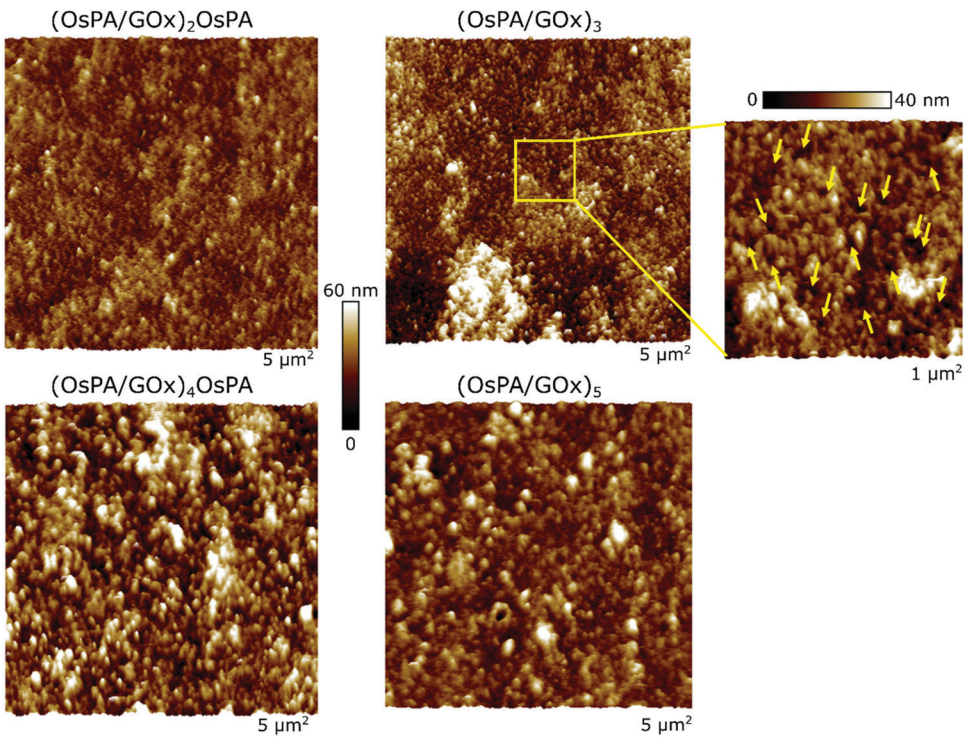

Fig. 5 *In situ* AFM topography images of the $(OsPA/GOx)_n$@Pi,HIS samples taken at different deposition layers with OsPA (left column) or GOx (right column) as the outermost layer; scanned area of 5 μm^2, height range 60 nm. A zoomed 1 μm^2 image of the $(OsPA/GOx)_3$ sample is also shown (height range 40 nm), with a structure presenting voids (some of them indicated by arrows) compatible with the globular structure proposed from DLS results.

Conclusions

The construction of thin layer films on interfaces involving proteins has seen intensive activity due to its application in diverse fields such as catalysis, biotechnology, and medical devices. In particular, the assembly of polyelectrolytes and proteins presents some limitations compared to construction from oppositely charged polyelectrolytes since proteins present a low conformational entropy and heterogeneous spatial charge distribution,[14] therefore the successful construction of the assembly heavily relies on the polyelectrolyte, where the pH, ionic strength and type of ions play a crucial role in its conformation. In this work, OsPA@Pi,HIS shows the formation of aggregates in solution with a bimodal distribution with particles of 7 and 16 nm diameter; once it is adsorbed on a surface, the formation of a globular structure can be observed by AFM. These structures linearly grow when they are combined with GOx, and efficient catalytic currents are obtained. To establish how phosphate ions and the high ionic strength conditions affect the growth of the film, experiments at high ionic strength without phosphate and experiments at low ionic strength with phosphate were carried out. No aggregates over 3 nm are observed by DLS examination for the OsPA@HIS solution; the assembly construction with this solution shows a negligible signal in electrochemical and QCM experiments, indicating a strong screening effect for the electrostatic interaction between the polyelectrolyte and the enzyme. Using an OsPA@Pi,LIS solution, a random behavior is observed during the film buildup. These results are in accordance with previous results observed by other authors where phosphate ions strip the already deposited layers.

Regarding the assembly of the protein, DLS experiments of the GOx solution in the presence of phosphate and a high concentration of NaCl do not show any aggregation effect, showing a similar hydrodynamic radius to that in pure water.[41] However, a notable change in the amount of enzyme adsorbed depending on the presence of phosphate in solution can be observed, which can decrease four times in its presence. Two effects can explain this difference: on the one hand, the presence of phosphate in solution has a rinsing effect as it was previously observed, and on the other hand, the film features can induce changes in the GOx adsorption process. The increase in the amount of adsorbed GOx can be interpreted through two type of interactions. One related to the fact that low ionic strength allows more electrostatic interactions between negatively charged glucose oxidase and the globular positively charged polyallylamine osmium complex on the surface, and the other, the phosphate ability to interact with basic amino acid residues such as lysine and arginine.[43] Considering this hypothesis, the phosphate in the film can interact with the GOx through its basic amino residues, improving the interaction between the polyelectrolyte and the enzyme. In this sense, phosphate ions have been shown to be suitable promoters to stabilize several proteins onto electrodes due to their ability to interact with amino groups.[25,26,39]

The increase in the amount of GOx adsorbed increases the catalytic current, but it is not directly proportional, suggesting that the OsPA does not efficiently connect part of the enzyme. For the system built from OsPA@Pi,HIS and GOx@H_2O, the ratio between osmium redox centers and GOx is around 10, representing an optimum relationship for the generation of the catalytic current, which is comparable to other efficient systems built from LbL assemblies based on the use of surfactants[10] or ferrocene modified linear PEI.[44]

It is well known that the electrostatic interaction between proteins and polyelectrolytes is the main driving force used for the construction of LbL films, a fact already observed for other protein–polyelectrolyte combinations.[25] The results presented here demonstrate how the environment surrounding each of the components used in the construction of the multilayer system can affect the amount of adsorbed material, its film structure and, finally, the electrochemical response, increasing the available tools for the construction of new nanoarchitectures.

Conflicts of interest

The authors declare no conflict of interest.

Acknowledgements

This work was supported by the following institutions: Universidad de Buenos Aires (UBACYT 20020170100341BA), ANPCYT (BID PICT 2015-0801, 2016-1680, 2017-1523), and CONICET (PIP-0370). Daniele Zappi thanks the Erasmus + ICM program for supporting his stay at Universidad de Buenos Aires.

References

1 V. Selin, V. Albright, J. F. Ankner, A. Marin, A. K. Andrianov and S. A. Sukhishvili, *ACS Appl. Mater. Interfaces*, 2018, **10**, 9756–9764.
2 D. Gaddes, H. Jung, A. Pena-Francesch, G. Dion, S. Tadigadapa, W. J. Dressick and M. C. Demirel, *ACS Appl. Mater. Interfaces*, 2016, **8**, 20371–20378.
3 S. S. Sha'rani, E. Abouzari-Lotf, M. M. Nasef, A. Ahmad, T. M. Ting and R. R. Ali, *J. Power Sources*, 2019, **413**, 182–190.
4 M. L. Cortez, A. Lorenzo, W. Marmisollé, C. von Bilderling, E. Maza, L. I. Pietrasanta, F. Battaglini, M. Ceolín and O. Azzaroni, *Soft Matter*, 2018, **14**, 1939–1952.
5 S. C. Feifel, A. Kapp, R. Ludwig and F. Lisdat, *Angew. Chem., Int. Ed.*, 2014, **53**, 5676–5679.
6 M. L. Cortez, N. De Matteis, M. Ceolín, W. Knoll, F. Battaglini and O. Azzaroni, *Phys. Chem. Chem. Phys.*, 2014, **16**, 20844–20855.
7 V. Flexer, E. S. Forzani, E. J. Calvo, S. J. Ludueña and L. I. Pietrasanta, *Anal. Chem.*, 2006, **78**, 399–407.
8 E. J. Calvo, V. Flexer, M. Tagliazucchi and P. Scodeller, *Phys. Chem. Chem. Phys.*, 2010, **12**, 10033–10039.
9 K. Ariga, Y. Yamauchi, G. Rydzek, Q. Ji, Y. Yonamine, K. C.-W. Wu and J. P. Hill, *Chem. Lett.*, 2014, **43**, 36–68.
10 M. L. Cortez, A. L. Cukierman and F. Battaglini, *Electrochem. Commun.*, 2009, **11**, 990–993.

11 M. Lösche, J. Schmitt, G. Decher, W. G. Bouwman and K. Kjaer, *Macromolecules*, 1998, **31**, 8893–8906.
12 W. Dressick, K. Wahl, N. Bassim and R. Stroud, *Langmuir*, 2012, **28**, 15831–15843.
13 A. Mafi, D. Hu and K. C. Chou, *Langmuir*, 2017, **33**, 7940–7946.
14 A. vander Straeten, A. Bratek-Skicki, A. M. Jonas, C.-A. Fustin and C. Dupont-Gillain, *ACS Nano*, 2018, **12**, 8372–8381.
15 P. Andreozzi, E. Diamanti, K. R. Py-Daniel, P. R. Cáceres-Vélez, C. Martinelli, N. Politakos, A. Escobar, M. Muzi-Falconi, R. Azevedo and S. E. Moya, *ACS Appl. Mater. Interfaces*, 2017, **9**, 38242–38254.
16 A. C. Santos, F. J. Veiga, J. A. D. Sequeira, A. Fortuna, A. Falcão, I. Pereira, P. Pattekari, C. Fontes-Ribeiro and A. J. Ribeiro, *Analyst*, 2019, **144**, 2062–2079.
17 A. G. Grigoras, *Nanomedicine*, 2017, **13**, 2425–2437.
18 X. Han, M. Han, L. Ma, F. Qu, R.-M. Kong and F. Qu, *Talanta*, 2019, **194**, 55–62.
19 T. S. Bronder, A. Poghossian, M. P. Jessing, M. Keusgen and M. J. Schöning, *Biosens. Bioelectron.*, 2019, **126**, 510–517.
20 Q. Xue, Y. Ding, Y. Xue, F. Li, P. Chen and Y. Chen, *Carbon N. Y.*, 2018, **139**, 137–144.
21 M. Fernández-Fernández, M. Á. Sanromán and D. Moldes, *Biotechnol. Adv.*, 2013, **31**, 1808–1825.
22 L. Paltrinieri, K. Remmen, B. Müller, L. Chu, J. Köser, T. Wintgens, M. Wessling, L. C. P. M. de Smet and E. J. R. Sudhölter, *J. Membr. Sci.*, 2019, **587**, 117162.
23 M. R. Awual and A. Jyo, *Water Res.*, 2009, **43**, 1229–1236.
24 G. Laucirica, W. A. Marmisollé and O. Azzaroni, *Phys. Chem. Chem. Phys.*, 2017, **19**, 8612–8620.
25 D. A. Capdevila, W. A. Marmisollé, F. J. Williams and D. H. Murgida, *Phys. Chem. Chem. Phys.*, 2013, **15**, 5386–5394.
26 C. Peng, J. Liu, Y. Xie and J. Zhou, *Phys. Chem. Chem. Phys.*, 2016, **18**, 9979–9989.
27 S. E. Herrera, M. L. Agazzi, M. L. Cortez, W. A. Marmisollé, C. Bilderling and O. Azzaroni, *Macromol. Chem. Phys.*, 2019, 1900094.
28 M. L. Cortez, M. Ceolín, L. Cuellar Camacho, E. Donath, S. E. Moya, F. Battaglini and O. Azzaroni, *ACS Appl. Mater. Interfaces*, 2017, **9**, 1119–1128.
29 M. L. Cortez, W. Marmisolle, D. Pallarola, L. I. Pietrasanta, D. H. Murgida, M. Ceolín, O. Azzaroni and F. Battaglini, *Chem.–Eur. J.*, 2014, **20**, 13366–13374.
30 M. L. Cortez, D. Pallarola, M. Ceolín, O. Azzaroni and F. Battaglini, *Chem. Commun.*, 2012, **48**, 10868–10870.
31 C. Danilowicz, E. Cortón and F. Battaglini, *J. Electroanal. Chem.*, 1998, **445**, 89–94.
32 I. Boron, S. Wirth and F. Battaglini, *Electroanalysis*, 2017, **29**, 616–621.
33 D. S. Salloum and J. B. Schlenoff, *Biomacromolecules*, 2004, **5**, 1089–1096.
34 V. Flexer, K. F. E. Pratt, F. Garay, P. N. Bartlett and E. J. Calvo, *J. Electroanal. Chem.*, 2008, **616**, 87–98.
35 A. Liu and J. Anzai, *Langmuir*, 2003, **19**, 4043–4046.
36 S. E. Herrera, M. L. Agazzi, M. L. Cortez, W. A. Marmisollé, M. Tagliazucchi and O. Azzaroni, *ChemPhysChem*, 2019, **20**, 1044–1053.
37 D. Kovačević, S. van der Burgh, A. de Keizer and M. A. Cohen Stuart, *J. Phys. Chem. B*, 2003, **107**, 7998–8002.
38 M. Salomäki, P. Tervasmäki, S. Areva and J. Kankare, *Langmuir*, 2004, **20**, 3679–3683.
39 W. A. Marmisollé, J. Irigoyen, D. Gregurec, S. Moya and O. Azzaroni, *Adv. Funct. Mater.*, 2015, **25**, 4144–4152.
40 J. J. Iturri Ramos, S. Stahl, R. P. Richter and S. E. Moya, *Macromolecules*, 2010, **43**, 9063–9070.
41 E. Piccinini, D. Pallarola, F. Battaglini and O. Azzaroni, *Chem. Commun.*, 2015, **51**, 14754–14757.
42 F. Caruso, D. N. Furlong, K. Ariga, I. Ichinose and T. Kunitake, *Langmuir*, 1998, **14**, 4559–4565.
43 M. Gruber, P. Greisen, C. M. Junker and C. Hélix-Nielsen, *J. Phys. Chem. B*, 2014, **118**, 1207–1215.
44 N. P. Godman, J. L. DeLuca, S. R. McCollum, D. W. Schmidtke and D. T. Glatzhofer, *Langmuir*, 2016, **32**, 3541–3551.

